Solution of the Holstein equation of radiation trapping by the geometrical quantization technique. III. Partial frequency redistribution with Doppler broadening

N. N. Bezuglov and A. K. Kazansky
Physics Institute, St. Petersburg University, Ulianovskaya 1, 198904 St. Petersburg, Russia

F. Fuso and M. Allegrini*
INFM, Dipartimento di Fisica, Università di Pisa, Via F. Buonarroti 2, I-56127 Pisa, Italy
(Received 29 September 2000; published 7 March 2001)

We introduce an analytical method to investigate radiation trapping problems with Doppler frequency redistribution. The problem is formulated within the framework of the Holstein-Biberman-Payne equation. We interpret the basic integro-differential trapping equation as a generalized wave equation for a four-dimensional (4D) classical system (an associated quasiparticle). We then construct its analytical solution by a semiclassical approach, called the geometrical quantization technique (GQT). Within the GQT, it is shown that the spatial and frequency variables can be separated and that the frequency part of the excited atom distribution function obeys a stationary Schrödinger equation for a perturbed oscillator. We demonstrate that there is a noticeable deviation of the actual spectral emission profile from the Doppler line in the region of small opacities. The problem of calculating the spatial mode structure and the effective radiation trapping factors is reduced to the evaluation of wave functions and quantized energy values of the quasiparticle confined in the vapor cell. We formulate the quantization rules and derive the phase factors, which allow us to obtain analytically the complete spectrum of the trapping factors in 1D geometries (layer, cylinder, sphere) and other (2D and 3D) geometries when the separation of space variables is possible. Finally, we outline a possible extension of our method to treat radiation trapping effects for more general experimental situations including, for instance, a system of cold atoms.

DOI: 10.1103/PhysRevA.63.042703 PACS number(s): 32.80.−t, 32.50.+d, 03.65.Sq

I. INTRODUCTION

In an optically thick vapor, a resonant photon can be ''trapped,'' so that it escapes from the vapor cell only after several subsequent absorption-emission processes by the vapor atoms [1,2]. This radiation trapping process is an important part of various physical phenomena, such as plasmas [3] and optical engineering problems [2]. Under laboratory conditions [4,5], the radiation trapping can strongly influence the spectral and temporal features of the radiation emerging from the cell and should be carefully considered in the quantitative analysis of experimental data [2,3,6] involving resonance radiation. However, solving the integro-differential equations describing the radiation trapping is a difficult mathematical problem, even in the most simple case of a two-level atom model with the assumption of complete frequency redistribution (CFR) for reemitted photons [3,7]. The main difficulty is due to divergence of the mean free path of the photons [3], which prevents any approximation of the integral trapping equations by a local diffusion equation of the Fokker-Plank type. Despite the intensive investigations during the past 50 years, no universally applicable analytical solution could be found. Even the study of the elementary one-dimensional geometries (infinite layer, infinite cylinder, sphere) of the vapor cell has resulted in a substantial number of very specific approximate techniques for different astrophysical and physical problems [2,8,9].

Recently, we have introduced [10,11] a universal, very accurate (albeit approximate) *analytical* method for solving the Holstein radiation trapping equation (also known as the Biberman-Holstein equation), the so-called geometrical quantization technique (GQT). The GQT was developed for the investigation of integral rate equations for the excited-state density in vapor cells of various shapes under the assumption of CFR. The GQT exploits the mathematical equivalence of the Holstein equation with the Schrödinger equation of a classical Hamiltonian system (also known as a quasiparticle), subjected to the canonical quantization [12]. Within the GQT, one obtains the mode structure and the radiation escape factors as the wave functions and the eigenvalues of the Schrödinger-like equation. In the present paper, we extend the GQT to situations with partial frequency redistribution (PFR) of reemitted photons. We restrict ourselves to the case in which the redistribution function is due to the Doppler effect only, for which the abbreviation DFR is used hereafter. This allows us to give a closed and relatively compact presentation of the GQT.

With the developed analytical technique, we confirm some conclusions derived previously from numerical studies [13–15] or obtained with mixed analytical-numerical methods [16]. We show that the deviations between the trapping factors evaluated within the CFR assumption and the data obtained for the case of DFR are *always* within 12% margins. At the same time, we demonstrate that the actual spectral emission profiles in the lowest eigenmodes (with respect to the frequency variable) can deviate considerably from the Doppler profile. We discuss also the higher-mode relaxation effects, addressing the temporal behavior of the escaping ra-

*On sabbatical leave from Dipartimento di Fisica della Materia e Tecnologie Fisiche Avanzate, Università di Messina, Salita Sperone 31, I-98166 Sant'Agata, Italy.

diation in after-glow experiments. An anomalous structure in the time dependence of the radiation intensity during the first stage of the emission of trapped light is shown to be due to some competing processes.

The paper is organized as follows. In Sec. II, the master equation determining the dynamics of radiation trapping processes with the Doppler frequency redistribution function is discussed. In Sec. III, the reduction of the master equation to the form of a 4D (one frequency and three spatial variables) generalized wave equation is described. In Sec. IV, the master equation is analyzed and the explicit representations both for the trapping factors and for the frequency distribution functions in the modes are obtained for the case of an infinitely extended medium. In Sec. V, we introduce the GQT for the study of finite gas cells of various geometries. This technique has been shown to be rather accurate [10,11] for the case of CFR; its accuracy for DFR is discussed in detail here. The GQT relates the radiation trapping problem to the consideration of the motion of a classical quasiparticle confined in the cell. It is shown that the GQT allows one to separate effectively the frequency and spatial variables. The generalized quantization rules are formulated and the relevant phase factors are calculated. Finally, we apply the GQT for the construction of semiclassical analytical representations of the effective radiation constants and the frequency distribution functions in the eigenmodes. Section VI contains a description of the ready-to-use recipes for evaluating both the trapping factors and the emission profiles. We compare the results obtained within the present method with numerical data of previous investigations and demonstrate that our results are accurate within 2–4 % for the fundamental mode and even better ($<0.5\%$) for higher-order modes. To emphasize some specific features of the radiation transfer with PFR, we perform a special study of the temporal dependence of the emergent radiation intensity in an after-glow experiment. Some possibilities for further development of the described approach are outlined. Section VII summarizes the main aspects of the GQT and its relation to the general PFR problems. A semiclassical discussion, aimed at confirming the idea of the frequency and spatial variables separation, is relegated to Appendix A. In order to minimize mathematical details, references will be made to the original literature whenever possible.

We would suggest that those readers interested only in the ready-to-use analytical recipes for an efficient calculation of the trapping factors restrict themselves to Sec. II and Sec. VI.

II. FORMULATION OF THE PROBLEM

The fundamental problem we address in this paper can be illustrated by the basic equations [4,2] mastering the time evolution of the frequency-dependent density function of the excited atoms $n^*(\vec{r},\nu,t)$ over the space coordinate $\vec{r}$ and the frequency ν (which is directly related to the velocity distribution of the atoms in the case of Doppler broadening):

$$\frac{\partial n^*(\vec{r},\nu,t)}{\partial t} = -A_{21}n^*(\vec{r},\nu,t) - A_{21}W(\vec{r})n^*(\vec{r},\nu,t) + A_{21}\int_{-\infty}^{\infty} d\nu' \int_{\Omega} d^3r' G_{\nu\nu'}(|\vec{r}-\vec{r}'|) \times n^*(\vec{r}',\nu',t) + S(\vec{r},\nu,t). \quad (1)$$

The product $A_{21}n^*(\vec{r},\nu,t)\Delta V d\nu$ gives an amount of photons spontaneously emitted per one second within the frequency interval $[\nu;\nu+d\nu]$ by the excited atoms contained in the volume ΔV; A_{21}^{-1} is the lifetime of the excited state with respect to its spontaneous decay;[1] $W(\vec{r})$ is the dimensionless intensity of the excited atoms quenching by unspecified processes of nonradiative decay. Here we assume that the function $W(\vec{r})$ provides the vanishing of the density function $n^*(\vec{r},\nu,t)$ outside a given space cell Ω.[2] The propagator $G_{\nu\nu'}(|\vec{r}-\vec{r}'|)$ describes the photon transfer from an emitting atom to an absorbing one. The term $S(\vec{r},\nu,t)$ provides a (nonstationary) source of the excited atoms. In Eq. (1), we do not consider explicitly the polarization and alignment phenomena discussed by D'yakonov and Perel' [17]. These phenomena can be studied within the present approach by treating $n^*(\vec{r},\nu,t)$ not as a scalar quantity, but as the corresponding spherical tensor (see also [13]).

The problem we discuss is determined by the following formula for the propagator $G_{\nu\nu'}(\rho)$:

$$G_{\nu\nu'} = \overline{\kappa} R_{\nu\nu'} \tilde{G}_{\nu'}(\rho) \quad \text{with}$$

$$\tilde{G}_{\nu'}(\rho) = \frac{1}{4\pi\rho^2}\exp[-\rho\kappa(\nu')], \quad \overline{\kappa} \equiv \int_{-\infty}^{\infty} d\nu\, \kappa(\nu), \quad (2)$$

where $R_{\nu\nu'}$ is the angle-averaged frequency redistribution function and $\kappa(\nu)$ is the spectral absorption coefficient. The universal identity [4]

$$\overline{\kappa}\int_{-\infty}^{\infty} d\nu\, R_{\nu\nu'} = \kappa(\nu') \quad (3)$$

implies that the effective photon absorption occurs only via the photon reemission with changed frequency.

For the case of pure Doppler broadening, the conventional representations for the functions involved are as follows [4]:

$$\kappa(\nu) = \kappa^{(D)}(\nu) \equiv \kappa_0^{(D)}\exp(-\nu^2), \quad \overline{\kappa} = \sqrt{\pi}\kappa_0^{(D)}, \quad (4)$$

$$R_{\nu\nu'} = \tfrac{1}{2}\mathrm{erf}(\max\{|\nu|,|\nu'|\}). \quad (5)$$

The Doppler absorption coefficient $\kappa_0^{(D)}$ in the center of the spectral line and the dimensionless reduced frequency ν,

[1] In what follows, we set $A_{21}=1$, fixing the natural for the problem time scale.

[2] This allows one to integrate over the infinite three-dimensional space in Eq. (1) by setting W very large outside the vapor cell [10]. See also Sec. V and Appendix A.

measured from the line center in the Doppler width units, $\Delta\nu^{(D)}$, are used in Eqs. (4) and (5). It should be noted that nontrivial evolution occurs only for the even, over-the-frequency variable, component of the function $n^*(\vec{r},\nu,t)$.

III. REDUCTION OF THE TRAPPING EQUATION

First, let us convert the trapping integral equation (1) with the Doppler redistribution function (5) in the form of a generalized differential (wave) equation. Considering the frequency redistribution kernel $R_{\nu\nu'}$, we can easily verify the following identity [4]:

$$\frac{\partial}{\partial\nu}\exp(\nu^2)\frac{\partial}{\partial\nu}R_{\nu\nu'}=-\frac{1}{\sqrt{\pi}}[\delta(\nu-\nu')+\delta(\nu+\nu')]. \quad (6)$$

Equation (6) can be represented in the form

$$\left[-\frac{1}{2}\frac{\partial^2}{\partial\nu^2}+\frac{1+\nu^2}{2}\right]\exp\left(\frac{\nu^2}{2}\right)R_{\nu\nu'}$$
$$=\frac{1}{2\sqrt{\pi}}\exp\left(-\frac{\nu^2}{2}\right)[\delta(\nu-\nu')+\delta(\nu+\nu')]. \quad (7)$$

Hence, the kernel $R_{\nu\nu'}$ in Eq. (5) is directly related to the Green function of the second-order differential operator of quantum oscillator type.

In Eq. (1), the integral operator over space variables can be converted into the form of a generalized differential operator. Formally, the general integral convolution operator $\hat{G}$

$$\hat{G}f(\vec{r})=\int_{R^3}d^3r'G(|\vec{r}-\vec{r}'|)f(\vec{r}') \quad (8)$$

is interpreted as the corresponding operator function over the momentum operator $\hat{\vec{p}}=-i\vec{\nabla}$ [10,11], and so it can be rewritten as follows [10]:

$$\int_{R^3}d^3r'G(|\vec{r}-\vec{r}'|)f(\vec{r}')=G^{(F)}(-i\vec{\nabla})f(\vec{r}),$$

$$G^{(F)}(\vec{p})\equiv\int_{R^3}d^3r'G(\vec{r}')\exp(i\vec{p}\vec{r}'). \quad (9)$$

In the case of Eq. (1), the representation for the Fourier transform $G^{(F)}(\vec{p})$ of the kernal function $\tilde{G}_{\nu'}$, Eq. (2), is well known [8]:

$$\tilde{G}^{(F)}_{\nu'}(\vec{p})=\frac{1}{p}\arctan\left[\frac{p}{\kappa^{(D)}(\nu')}\right], \quad p=|\vec{p}|. \quad (10)$$

The spatial isotropy of the task under consideration manifests itself in the independence of the function $\tilde{G}^{(F)}_{\nu'}$ of the momentum direction. With the identities Eqs. (7), (9), and (10), the trapping master equation (1) turns out to exhibit the structure of a diffusion-type equation:

$$\hat{L}_\nu\left[\frac{\partial}{\partial t}+1+W(\vec{r})\right]\tilde{n}^*(\vec{r},\nu,t)=\Phi(-i\vec{\nabla},\nu)\tilde{n}^*(\vec{r},\nu,t)$$
$$+\hat{L}_\nu S(\vec{r},\nu,t), \quad (11)$$

$$\hat{L}_\nu=-\frac{1}{2}\frac{\partial^2}{\partial\nu^2}+\frac{1+\nu^2}{2},$$

$$\Phi(\vec{p},\nu)=\frac{\kappa^{(D)}(\nu)}{|\vec{p}|}\arctan\left[\frac{|\vec{p}|}{\kappa^{(D)}(\nu)}\right], \quad (12)$$

$$\tilde{n}^*(\vec{r},\nu,t)=\exp\left(\frac{\nu^2}{2}\right)n^*(\vec{r},\nu,t). \quad (13)$$

Equation (11) is the starting point for our further analytical treatment of the trapping problem.

From an experimental standpoint, the determination of the trapping factors g_j [7] is of particular importance. These factors are the eigenvalues for the spectral problem related to the trapping equation [7]:

$$n^*(\vec{r},\nu,t)=\Psi_j^*(\vec{r},\nu)\exp(-\lambda_j t), \quad g_j=1/\lambda_j. \quad (14)$$

The functions Ψ_j^* (the eigenmodes) with the corresponding eigenvalues λ_j (effective radiation rate constants) can be obtained from Eq. (11) by setting $\partial/\partial t\to-\lambda_j$ and omitting the source function S:

$$\hat{L}_\nu[-\lambda_j+1+W(\vec{r})]\tilde{\Psi}_j^*(\vec{r},\nu)=\Phi(-i\vec{\nabla},\nu)\tilde{\Psi}_j^*(\vec{r},\nu),$$

$$\tilde{\Psi}_j^*=\exp\left(\frac{\nu^2}{2}\right)\Psi_j^*. \quad (15)$$

The trapping (Holstein) factor g_j gives the rate of absorption/reemission processes for a photon in the jth mode. Note that an exhaustive solution of the trapping Eq. (1) via the Fourier method [2,7] requires us to find the complete set (spectrum) of Ψ_j^* and λ_j.

IV. EIGENMODES IN INFINITE SPACE

Let us consider the eigenvalue problem expressed by Eq. (15) in the entire infinite space. This implies omitting the extra quenching of excited atoms W (see footnote 2). The main feature of Eq. (15) with $W=0$ is that it allows an *exact* separation of the spatial and frequency variables:

$$\Psi_j^*(\vec{r},\nu)=\exp(i\vec{p}\vec{r})\varphi_p(\nu), \quad \varphi_p(\nu)=\exp\left(-\frac{\nu^2}{2}\right)\tilde{n}_p(\nu), \quad (16)$$

$$\left(-\frac{1}{2}\frac{\partial^2}{\partial\nu^2}+\frac{1}{2}\nu^2+\frac{1}{(1-E)}V_p(\nu)\right)\tilde{n}_p(\nu)$$
$$=\frac{1+E}{2(1-E)}\tilde{n}_p(\nu) \quad \text{with} \quad p=|\vec{p}|, \quad (17)$$

$$E=\lambda_j,$$

$$V_p(\nu)=1-\Phi(\vec{p},\nu)$$
$$=1-\frac{\kappa_0^{(D)}\exp(-\nu^2)}{p}\arctan\left[\frac{p}{\kappa_0^{(D)}}\exp(\nu^2)\right]. \quad (18)$$

The function $\varphi_p(\nu)$ is the real spectral emission profile, while the function $\tilde{n}_p(\nu)$ can be regarded as a modified emission profile. Problem (17) can be classified as a perturbed oscillator eigenproblem, though the spectral parameter $E=\lambda_j$ enters it in an intricate way. It should be noted that Eq. (17) can be considered as a wave equation and its solutions result in obtaining the set of dispersion curves $E=E_n(p)$ and corresponding p-dependent eigenfunctions $\tilde{n}_p(\nu)$.

First, we study the range of very large ''reduced opacities''[3] $\tau_r\equiv\kappa_0^{(D)}p^{-1}\to\infty$. In this limit $V_p(\nu)\to 0$ and one obtains, as the lowest approximation, the stationary Schrödinger equation for the oscillator [18] with its frequency and mass equal to unity:

$$\left(-\frac{1}{2}\frac{\partial^2}{\partial\nu^2}+\frac{1}{2}\nu^2\right)\tilde{n}_{p=0}(\nu)=\Lambda\tilde{n}_{p=0}(\nu),\quad \Lambda=\frac{1+E}{2(1-E)}. \quad (19)$$

Consequently, $\Lambda_n=n+1/2$, which means that

$$E_{2k}=\frac{n}{n+1},\quad n=2k. \quad (20)$$

Since we consider only even spectral distribution functions, we take only even values of the ''internal'' state number n. The frequency eigenfunctions are the well-known oscillator eigenfunctions [18]

$$|n\rangle=\tilde{n}_{p=0}^{(n)}(\nu)$$
$$=H_n(\nu)$$
$$=(-1)^n\frac{1}{\pi^{1/4}}\frac{1}{\sqrt{2^n n!}}\exp\left(\frac{\nu^2}{2}\right)\frac{\partial^n}{\partial\nu^n}\exp(-\nu^2). \quad (21)$$

For the lowest eigenstate $n=0$, Eq. (20) gives $E_0=0$. This state (the fundamental mode) describes a stable solution of the radiation trapping problem. For $k>0$, the corresponding relaxation constants E_{2k} are in the same order of magnitude of the Einstein coefficient A_{21} and therefore the corresponding eigenmodes decay promptly. This means that, in the large opacities limit, when a remarkable number of reemission processes occur, only the Doppler distribution corresponding to the pure Gauss spectral line profile

$$\varphi_{p=0}^{(n=0)}(\nu)=\exp(-\nu^2/2)\tilde{n}_{p=0}^{(n=0)}(\nu)=\frac{1}{\pi^{1/4}}\exp(-\nu^2) \quad (22)$$

survives whatever the initial frequency distribution is. This statement was demonstrated numerically in [15].

To investigate the case of finite values of the reduced opacity $\tau_r=\kappa_0^{(D)}p^{-1}$, we can apply the perturbation theory and average Eq. (17) over the corresponding eigenfunction $H_n(\nu)$:

$$E_{2k}(p)=\frac{2k+\Delta_{2k}(p)}{1+2k},$$

$$\Delta_{2k}(p)\approx\Delta_{2k}^{(\mathrm{app})}(p)$$
$$=1-\int_{-\infty}^{\infty}d\nu\,H_{2k}^2(\nu)\frac{\kappa^{(D)}(\nu)}{p}\arctan\left[\frac{p}{\kappa^{(D)}(\nu)}\right]. \quad (23)$$

For the case of the lowest-frequency mode, $k=0$, we obtain

$$E_0(p)\approx\tilde{V}_D(p)$$
$$\equiv 1-\frac{1}{\sqrt{\pi}}\int_{-\infty}^{\infty}d\nu\exp(-\nu^2)\frac{\kappa^{(D)}(\nu)}{p}\arctan\left[\frac{p}{\kappa^{(D)}(\nu)}\right], \quad (24)$$

in full agreement with the conventional theory for the complete frequency redistribution case [10]. In the region of large values of $\tau_r(p\to 0)$, Eq. (23) has the following simple asymptotic representation [8]:

$$\Delta_{2k}(p)\simeq\frac{\sqrt{\pi}}{2^{2k+2}(2k)!}\frac{p}{\kappa_0^{(D)}}\left[\ln\left(\frac{\kappa_0^{(D)}}{p}\right)\right]^{2k-0.5}$$

when

$$\tau_r=\kappa_0^{(D)}p^{-1}\gg 1. \quad (25)$$

The form of the solutions for Eq. (11) [Eqs. (14) and (16)] implies that the eigenmodes describe the propagation of a free quantum-mechanical quasiparticle [10] with the momentum $\vec{p}$. This quasiparticle has an internal structure related to the variable ν. The quasiparticle energies $E_{2k}(p)$ depend on the state of the internal motion $(2k)$ and on the quasiparticle momentum p. The effective radiation decay rate constants $\lambda_{n,p}=E_n(p)$ correspond to different branches (classified by the quantum number n) of the dispersion curves for the wave equation (17). From this point of view, the spectral problem for the CFR approach can be reduced to the study of a structureless quasiparticle problem; the corresponding radiation constant $\lambda_p=E_0^{(\mathrm{CFR})}(p)=\tilde{V}_D(p)$ [Eq. (24)] is the kinetic energy of the quasiparticle [10].

The perturbation approach fails for the small reduced opacity region $\kappa_0^{(D)}p^{-1}\sim 1$, where $E_{2k}\to 1$ for all k. This limiting case $(p\to\infty)$ can be studied by setting

[3]In a finite volume, the momentum $p\sim L^{-1}$ and $\tau_r\simeq\tau=\kappa_0^{(D)}L$, where L is the characteristic size of the vapor cell. See also the quantization rules below, Eqs. (35), (40), and (42), connecting τ_r to the conventional opacity τ.

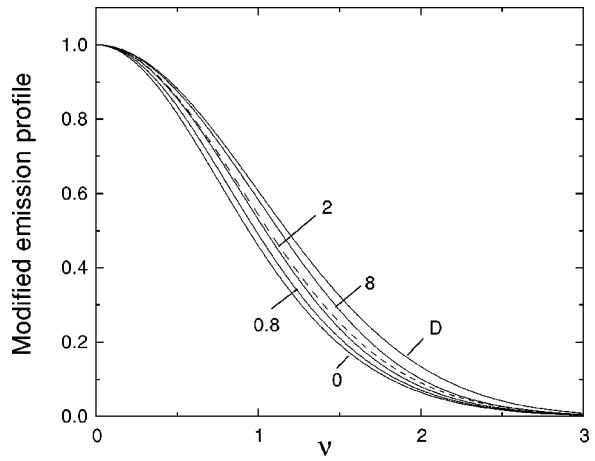

FIG. 1. Modified emission profiles $\tilde{n}_p^{(0)}(\nu)=\exp(\nu^2/2)\varphi_p^{(0)}(\nu)$ for different reduced opacities $\tau_r=\kappa_0^{(D)}p^{-1}$ (as marked close to each curve) in the case of the fundamental branch $n=0$. The Doppler profile $\exp(-\nu^2/2)$ (marked as D) corresponds to the complete frequency redistribution approach. The dashed curve with $\tau_r=2$ was calculated for the ground mode in the center of a layer by numerical methods [23].

$$E_{2k}(p)\simeq 1-\kappa_0^{(D)}p^{-1}\Gamma_{2k} \tag{26}$$

and rewriting Eq. (17) as a spectral problem for the coefficient Γ:

$$\left(-\frac{1}{2}\frac{\partial^2}{\partial\nu^2}+\frac{1}{2}\nu^2-\frac{\pi}{2\Gamma}\exp(-\nu^2)\right)\tilde{n}_{\tau\sim 0}(\nu)$$

$$=-\frac{1}{2}\tilde{n}_{\tau\sim 0}(\nu). \tag{27}$$

The solution $\tilde{n}_{\tau\sim 0}^{(n=0)}(\nu)$ of Eq. (27) for the fundamental branch is presented in Fig. 1 (the curve marked by 0), where the modified Doppler curve $\exp(-\nu^2/2)$ is also shown (the curve D). The corresponding Γ_0 value turns out to be 1.17, while in the CFR case the formula for the dispersion law $\tilde{V}_D(p)$, Eq. (24), gives $\Gamma^{(\mathrm{CFR})}=\pi/(2\sqrt{2})$. Consequently,

$$E_0(p)\simeq 1-1.17\frac{\kappa_0^{(D)}}{p},\quad \tilde{V}_D(p)\simeq 1-1.11\frac{\kappa_0^{(D)}}{p},$$

$$\tau_r=\kappa_0^{(D)}p^{-1}<1. \tag{28}$$

In Fig. 2, we demonstrate the properties of the ground mode ($n\equiv 0$) dispersion law $E_0(p)$ as a function of the reduced opacity $\kappa_0^{(D)}p^{-1}$. Although the spectral emission profile $\varphi_p^{(n=0)}(\nu)$ deviates considerably from the Doppler curve at small opacities (see Fig. 1), the difference between dispersion curves $\tilde{V}_D(p)$ (CFR approach, dashed line) and $E_0(p)$ (solid line) turns out to be hardly noticeable (the deviation is less than 12%), as seen in Fig. 2.

The energies $E_{2k}(p)$ are directly related to the spectral emission profile $\varphi_p(\nu)$. To show this, we project Eq. (17) on the zero-level oscillator eigenfunction $\langle 0|=H_0(\nu)$

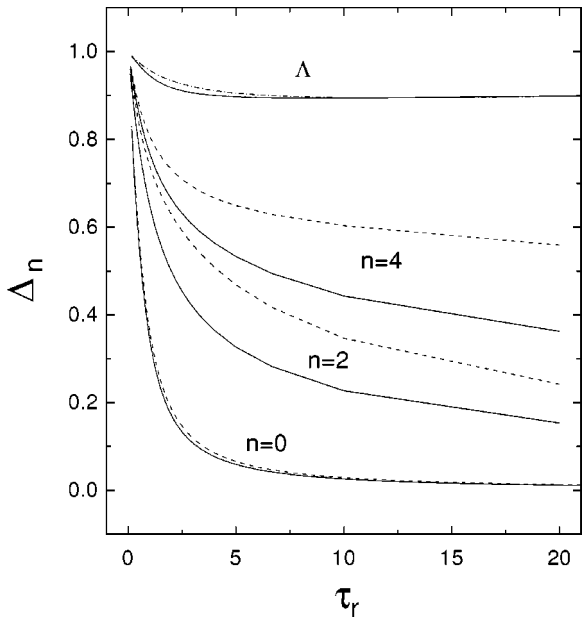

FIG. 2. $\Delta_n(p)$ (solid curves) as a function of the reduced opacity $\tau_r=\kappa_0^{(D)}p^{-1}$ for different even branches n (as marked close to each curve). The solid curve with $n=0$ corresponds to the ground mode branch and is identical to the dispersion law function $E_0(p)$. The dashed line with $n=0$ gives the $\tilde{V}_D(p)$ function related to the CFR approach and expressed by Eq. (24). The other dashed curves are obtained with the perturbation theory, Eq. (23). The solid line marked as Λ displays the ratio $E_0/\tilde{V}_D$ as a function of the reduced opacity. Its approximate expression, Eq. (41), is shown as a dashed-dotted line Λ.

$\sim\exp(-\nu^2/2)$ and take into account the identity $\langle 0|2\hat{L}_\nu=\langle 0|$ [see Eq. (19)]. We obtain

$$E_{2k}(p)=1-\frac{1}{C_{2k}}\int_{-\infty}^{\infty}d\nu\,\varphi_p^{(2k)}(\nu)\frac{\kappa^{(D)}(\nu)}{p}$$

$$\times\arctan\left[\frac{p}{\kappa^{(D)}(\nu)}\right],$$

$$C_{2k}=\int_{-\infty}^{\infty}d\nu\,\varphi_p^{(2k)}(\nu), \tag{29}$$

where C_{2k} is the normalization constant for the emission profile in the $2k$th dispersion branch. Thus, the difference between the trapping factors $\lambda_j=E(p)$ for the CFR case [Eq. (24)] and for the PFR case [Eq. (29)] occurs due to the spectral emission profiles $\varphi_p^{(2k=0)}(\nu)$, which are created by radiation transfer processes within the vapor cell.

V. TRAPPING FACTORS FOR A FINITE VAPOR CELL

The discussion of the spectral profiles $\varphi_p^{(2k)}(\nu)$ in infinite space given above provides a basis for further discussion of radiation trapping in a finite cell Ω. To describe the radiation processes in a cell, we set the quenching rate $W(\vec{r})=W_\Omega$ equal to infinity outside the vapor cell Ω and to zero inside

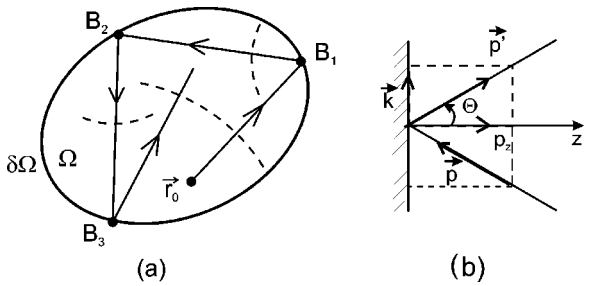

FIG. 3. Sketch of the quasiparticle billiard-type trajectory in the vapor cell volume. The dashed lines in (a) indicate the positions of the wave fronts after successive reflections (at points B_1, B_2, and B_3). In (b), the quasiparticle reflection from a plane potential wall is shown.

Ω. As $n^*(\vec{r},\nu,t)=0$ at any place where $W_\Omega=\infty$, the integral in Eq. (1) can be extended to the entire R^3 space. In this section and in Appendix A, we show that the jump of W_Ω at the vapor cell boundary $\partial\Omega$ entails the quasiparticle elastic reflections with the absolute magnitude of the momentum $p=|\vec{p}|$ being conserved. A typical quasiparticle trajectory has a billiard-type structure and consists of straight lines confined inside Ω (see Fig. 3).

Since only the absolute value p enters Eq. (17), the frequency dimension does not ''feel'' the existence of the cell boundary. This allows us to separate the spatial and frequency variables [compare with Eq. (16)]:

$$\Psi^*_{n,i}(\vec{r},\nu)\simeq\varphi_p^{(n)}(\nu)N_i(\vec{r}),\quad p=|\vec{p}_i|. \tag{30}$$

The semiclassical demonstration of this important ansatz is given in Appendix A. We emphasize that the frequency-dependent functions $\varphi_p^{(n)}(\nu)$ obey the same eigenproblem Eq. (17) as for the case of infinite space since p is constant. The quantity p is a characteristic of the spatial part of the problem and can be determined with the geometrical quantization technique [10,11] (see below). The semiclassical quantization rules introduce a set of spatial mode indices (quantum numbers) $i=\{i_1,\ldots,i_m\}$, which fix ''permitted'' values of the momentum $\vec{p}=\vec{p}_i$. It should be noted that the number m of these indices universally coincides with the space dimension.

The applicability range of the semiclassical treatment given in Appendix A deserves a discussion. Equation (A2) fails in the vicinity of a cell boundary where the quenching function W_Ω changes abruptly. It is shown in [10,19] that the size of the spatial regions where the semiclassical formulas need corrections (including caustic surfaces) turns out to be small enough. To illustrate the accuracy of the factorization approach, we give, in Sec. VI, an example of numerical calculation showing that Eq. (30) is rather accurate even in the stringent case of small opacity.

A. Geometric quantization rules

The mode factorization expressed by Eq. (30) leads to an integral equation for the total excited atom density $N_i(\vec{r})$ at the point $\vec{r}$ for a given eigenmode. Integrating both sides of Eq. (1) over the frequency ν, accounting for Eqs. (3), (30), and the eigenmode temporal dependence Eq. (14), we obtain

$$-\lambda_j N_i(\vec{r})=-W_\Omega N_i(\vec{r})+\frac{1}{C_n}\int_{R^3}d^3r'N_i(\vec{r}')\times\int_{-\infty}^{\infty}d\nu'\varphi_{p_i}^{(n)}(\nu')\kappa^{(D)}(\nu')\tilde{G}_{\nu'}(|\vec{r}-\vec{r}'|),$$
$$C_n=\int_{-\infty}^{\infty}d\nu'\varphi_{p_i}^{(n)}(\nu')\equiv 1\Leftrightarrow N_i(\vec{r})=\int_{-\infty}^{\infty}d\nu\,\Psi_j^*(\vec{r},\nu). \tag{31}$$

Equation (31) has the alternative form of a stationary wave equation [see Eqs. (9) and (10)]

$$\lambda_j N_i(\vec{r})=W_\Omega N_i(\vec{r})+V_n^{(p_i)}(-i\vec{\nabla})N_i(\vec{r}), \tag{32}$$

$$V_n^{(p_i)}(\vec{p})=1-\frac{1}{C_n}\int_{-\infty}^{\infty}d\nu\,\varphi_{p_i}^{(n)}(\nu)\frac{\kappa^{(D)}(\nu)}{|\vec{p}|}\arctan\left[\frac{|\vec{p}|}{\kappa^{(D)}(\nu)}\right]. \tag{33}$$

Analytical solutions of this equation are given in [10,11] within a modified semiclassical approach, the so-called geometric quantization technique (GQT). We briefly formulate the basic ideas of the GQT and apply them to the study of Eq. (15).

First, Eq. (32) is a 3D projection of the general Eq. (15) and it leads to the same billiard-type construction of the quasiparticle trajectories as described in [11]. Indeed, the classical Hamiltonian $H^{(3D)}$

$$H^{(3D)}(\vec{p},\vec{r})=W_\Omega+V_n^{(p_i)}(\vec{p}), \tag{34}$$

corresponding to the wave equation (32) and governing the quasiparticle dynamics, includes the quenching rate constant W_Ω as its potential energy. The above-mentioned jumps of this quantity at the cell boundaries create a potential well confining the quasiparticle inside Ω. From a semiclassical point of view, we can relate the search for the eigensolutions of the wave equation (32) and the determination of the quasiparticle eigenstates by imposing appropriate quantization conditions. The standing-wave solutions for an electromagnetic wave in a ''resonator'' Ω can be treated in a similar manner.

For the one-dimensional case, the simplest Bohr-Sommerfeld quantization rule (BSR) [18] is adequate for extracting the quantized values p_i of the quasiparticle momentum. For instance, in a plane-parallel layer ($-L/2<z<L/2$), when $\vec{p}$ is oriented along the z axis, the BSR determines the magnitude of the momentum $p_z^{(i)}$ as follows [10]:

$$p_i=p_z^{(i)},\quad 2\int_{-L/2}^{L/2}p_i dz=2p_iL=2\pi l_z+2\Delta S(p_i),$$
$$i=l_z=0,1,\ldots, \tag{35}$$

where $2\Delta S$ is the phase jump due to the two reflections of the quasiparticle at the potential walls $z=-L/2$ and $z=L/2$.

A more sophisticated procedure based on the Einstein-Brillouin-Keller quantization conditions [20–22] is needed for the determination of the quantized trajectory configurations for 2D and 3D vapor cells [11].

All quantization conditions imply that, on a closed path Γ_r, the total phase shift for the wave front, including the shifts ΔS due to wall reflections and caustic surfaces shifts $\Delta S_{\rm cau}$, must add up to entire multiples of 2π,

$$\oint_{\Gamma_r} \vec{p}_i \cdot d\vec{r} - \sum_{(r)} \Delta S_{(r)} = 2\pi l_r . \tag{36}$$

The modal multi-index $i=\{l_r\}$ consists of a set of integer (quantum) numbers l_r for the topologically independent cycles Γ_r. As shown in [11], the system of resonance equations, Eq. (36), determines the absolute magnitude of the quasiparticle momentum p_i uniquely. The effective radiation constants $\lambda_{n,i}$ can be evaluated as the quasiparticle energy $H^{(3D)}$, Eq. (34), within Ω ($W_\Omega=0$):

$$\lambda_{n,i} = V_n^{(p_i)}(|\vec{p}_i|) \equiv E_n(p_i). \tag{37}$$

Note that both the superscript index p_i and the argument p in the function $V_n^{(p_i)}(|\vec{p}|)$ have the same magnitude p_i, and, in accordance with Eqs. (33) and (29), $V_n^{(p_i)}(p_i)$ is equal to $E_n(p_i)$. This fact gives a quite natural quantitative connection between the 4D and 3D descriptions of the quasiparticle system.

B. Phase factors

Until now, the spatial evolution of the quasiparticle has been considered independently from its motion with respect to the frequency variable. The topology of the semiclassical trajectories inside Ω is not related to the kinetic energy $V_n^{(p_i)}(p)$: for any function $V_n^{(p_i)}$ the trajectory is the same (for a given p_i) and consists of the segments of straight lines terminated at the reflection points belonging to the cell boundary $\partial\Omega$. However, the eigenvalues and eigenfunctions are sensitive to the kinetic-energy function $V_n^{(p_i)}$ as the phase factors $\Delta S_{(r)}$ entering Eqs. (36) are actually functionals of the emission profiles.

The phase jumps acquired by the quasiparticle wave function due to reflection of the classical particle from the boundary of the potential wall and from the caustics are discussed in detail in [10,11]. The magnitudes of $\Delta S_{\rm cau}$ are connected only to certain topological invariants of the trajectories [20] and can be evaluated explicitly [18]. The formula for computation of the phase shift ΔS acquired due to the quasiparticle reflection from a flat wall at an angle θ, as is shown Fig. 3(b), is derived in [11]. We restrict ourselves here to 1D geometries where the reflection angle θ can be set equal to zero. For the eigenproblem Eq. (32), we obtain [10]

$$\Delta S^{(n)}(p_i, \theta=0) = \frac{\pi}{2} - \frac{2}{\pi}\int_0^1 \ln\left(\frac{\tilde{V}(p_i) - \tilde{V}(p_i\rho)}{\tilde{V}(p_i/\rho) - \tilde{V}(p_i)} \right) \frac{1}{1-\rho^2} d\rho,$$

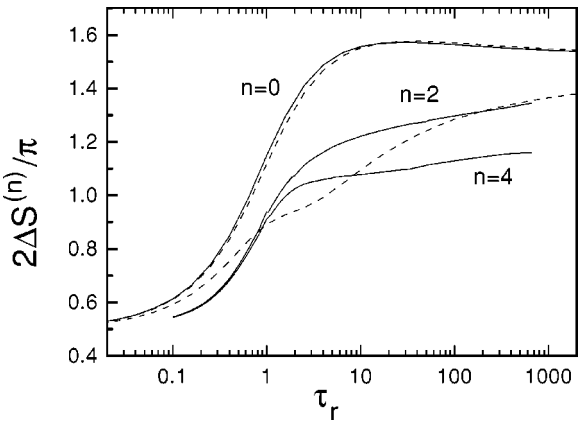

FIG. 4. Phase jump $2\Delta S^{(n)}/\pi$ (solid curves) plotted as a function of the reduced opacity $\tau_r = \kappa_0^{(D)} p^{-1}$. The quasiparticle is assumed to be reflected at the potential wall with the reflection angle $\theta=0$. Data correspond to various branches of the dispersion functions $E_n(p)$, as marked in the figure. The dashed lines are calculated within the perturbation theory.

$$\tilde{V}(p) \equiv V_n^{(p_i)}(p) \simeq E_n(p), \tag{38}$$

$$\Delta S_{\rm app}^{(n)}(p_i, \theta=0) = \frac{\pi}{2}[1 + \gamma_{\rm app}(p_i)],$$

where

$$\gamma_{\rm app}(p) = \frac{1}{2} p \frac{d}{dp} \ln\left(p \frac{d\tilde{V}(p)}{dp} \right). \tag{39}$$

It should be noted that the argument and the superscript index in the function $V_n^{(p_i)}(p_i\rho)$ entering the integrand of Eq. (38) are different. These quantities are close to each other in the vicinity of the point $\rho=1$ where the substitution $\tilde{V}(p_i\rho) = V_n^{(p_i)}(p_i\rho) \simeq E_n(p_i\rho)$ is valid [compare with the identity in Eq. (37)]. On the other hand, the principal contribution to the integral is due to the region near $\rho=1$ because of a strong singularity of the function $1/(1-\rho^2)$ in the integrand. Attention must be paid, in this regard, to the quite accurate approximate formula for $\Delta S^{(n)}$, Eq. (39), which was derived in [10] by exploring the mentioned singularity.

Equations (38) and (39) provide an analytical tool for evaluation of the phase jump $\Delta S^{(n)}$. In particular, if the energy $E_n(p)$ can be approximated as $E_n(p) \simeq a + bp^\gamma$ in the vicinity of p_i, then Eq. (39) gives $\Delta S^{(n)} = \pi/2(1+0.5\gamma)$. It follows from Eqs. (23), (25), and (26) that such a dependence of $E_n(p)$ is valid for small or large values of the reduced opacity with $\gamma_{\rm sm} = -1$ and $\gamma_{\rm lr} = 1$, respectively. Hence,

$$\Delta S^{(n)} = \pi/4, \quad \kappa_0^{(D)} p_i^{-1} \ll 1;$$

$$\Delta S^{(n)} = 3\pi/4, \quad \kappa_0^{(D)} p_i^{-1} \gg 1$$

independent of the branch index n. Figure 4 demonstrates (solid curves) the behavior of the phase jump $\Delta S^{(n)}$ due to the quasiparticle reflection from the cell walls as a function

of the reduced opacity. Due to the small difference between the magnitudes of the quasiparticle kinetic energy $E_{n=0}(p)$ (the DFR case) and $\tilde{V}_D(p)$ (the CFR approach), the corresponding phase jumps $\Delta S^{(n=0)}$ and $\Delta S^{(\mathrm{CFR})}$ (the dashed curve marked as $n=0$) are very similar.

Let us consider the quantization rule given by Eq. (36) for two practically important 1D cell geometries: cylinder and sphere of radius R. Since these problems are effectively one-dimensional, the momentum $\vec{p}$ is directed along the radius: $p=p_r$. The Bohr-Sommerfeld rule, Eq. (36), applied to the quasiparticle radial motion gives the quantization conditions determining the momentum p_i:

$$p_i=p_r^{(i)}, \quad 2p_iR=2\pi l_r+\Delta S^{(n)}(p_i,\theta=0)+\Delta S_{\mathrm{cau}},$$

$$i=l_r=0,1,\ldots, \tag{40}$$

$$\Delta S_{\mathrm{cau}}^{(\mathrm{Cl})}=\pi/2; \quad \Delta S_{\mathrm{cau}}^{(\mathrm{Sh})}=\pi, \quad \lambda_j=E_n(p_i), \quad j=\{n,i=l_r\},$$

where l_r is the radial quantum number. The phase jump ΔS_{cau} arises because the point $r=0$ in a cylinder or in a sphere is of caustic type (the particle is reflected at $r=0$ since formally its motion is restricted to the semiaxis $r\geqslant 0$); their magnitude $\Delta S_{\mathrm{cau}}^{(\mathrm{Cl})}$ (for a cylinder) and $\Delta S_{\mathrm{cau}}^{(\mathrm{Sh})}$ (for a sphere) can be obtained within the standard semiclassical framework [18].

VI. RESULTS AND DISCUSSION

Let us first formulate an explicit *recipe* for rapid calculation of the trapping factors $g_{n,i}=1/\lambda_{n,i}$ for the (n,i) mode $\Psi_{n,i}^*$ within the GQT. We stress that, due to the frequency redistribution, even in the simplest 1D geometries, a mode can be specified by, at least, two numbers, $j=\{n,i\}$. Namely, the index n corresponds to the frequency dependence of the modal function, whereas the index i accounts for its spatial dependence. For 2D and 3D geometries, the multi-index i incorporates other space quantum numbers [11].

The two types of indices correspond with the two stages in relaxation experienced by any initial distribution in the process of radiation trapping. First, the prompt relaxation of a primary created *frequency distribution* to that of the ground mode (with respect to the frequency variables, $n=0$) takes place. The corresponding rate constants can be evaluated as effective radiation decay constants $\lambda_{n,i}$ with even $n=2k$. The $\lambda_{n,i}^{-1}$ values (g factors) for $n\neq 0$ are close to the natural radiative lifetime and weakly depend on the opacity of the vapor cell.[4] Second, a *spatial relaxation* of radiation in the ground states $n=0$ occurs. At this stage, the modal function $\Psi_{n=0,i}^*=\varphi_{p_i}^{(n=0)}(\nu)\cdot N_i(\vec{r})$ carries the time-independent emission profile $\varphi_{p_i}^{(n=0)}(\nu)$, whereas the $g_{n=0,i}$ factors determine the spatial relaxation of excited atoms to the fundamental mode distribution $N_{i=0}(\vec{r})$.

To evaluate $\lambda_{n,i}$, one has to determine the quasiparticle quantized momentum values $p=p_i$ corresponding to the mode Ψ_j^*. This quantity can be obtained from the quantization rules, Eqs. (35) and (40). It is shown in Sec. V B that the phase jump ΔS entering Eq. (38) depends on the momentum p. On the other hand, Eqs. (35) and (40) exhibit a dependence of p on ΔS. In order to find self-consistent solutions for p_i, one can use the following iterative procedure.

(i) One chooses the modal index $j=\{2k,i\}$ of the mode for which the computations must be performed, and sets $l_z=i$ for a layer in Eq. (35) or $l_r=i$ for the curved geometries in Eq. (40). The fundamental mode corresponds to $n=i=0$ (the ground-state level for the quasiparticle).

(ii) We recommend using $\Delta S=\pi/2$ as an initial value for the phase jump.

(iii) With this value for ΔS, from Eqs. (35) and (40) one obtains p_i for the cell geometry under consideration.

(iv) With this p_i, one can compute a new value of ΔS using Eq. (38) (at the final step) or its approximation, Eq. (39) (at the first steps). As an income, this procedure needs the function $E_{2k}(p)$, which can be provided by Eq. (17). This equation is a regular quantum-mechanical stationary wave equation [18] for a perturbed oscillator and it routinely determines the $2k$th eigenvalue E_{2k}. The dependence E_{2k} on the momentum p appears via the function $V_p(\nu)$, which contains the quantity p as a parameter. Fortunately, for the most interesting case of the ground levels ($n=0$), the phase factor ΔS practically coincides with the phase ΔS^{CFR} (see the solid and dashed lines marked $n=0$ in Fig. 4), which can be evaluated from Eq. (39) or Eq. (38), the function E_0 being determined by the explicit formula given in Eq. (24).

(v) If the resulting value of ΔS deviates significantly from the previous one, one returns to step (iii) (typically, two or three iterations are enough).

(vi) Once a converged value of ΔS is obtained, p_i can be determined for the (n,i) mode.

(vii) The trapping factors g_j can then be evaluated according to Eq. (37), as $g_j=1/E_{2k}(p_i)$. As we mentioned above (Sec. IV), the function $E_0(p)$ is very close to the function $\tilde{V}_D(p)$, Eq. (24), for the CFR case (see also Fig. 2, curves $n=0$). The expression

$$E_0(p)=\Lambda(p)\tilde{V}_D(p), \quad \Lambda(p)=\frac{1+2.42\ln(1+0.0885/p)}{1+2.42\ln(1+0.113/p)} \tag{41}$$

approximates $E_0(p)$ within a 1% margin (see the curves marked Λ in Fig. 2). This approximation allows one to calculate the trapping factors $g_{n=0,i}$ (covering the fundamental mode case, $i=0$) for 2D and 3D geometries, using the GQT methods described in [11] by substitution of the energy $\tilde{V}_D(p)$ with the function $E_0(p)$.

(viii) The obtained p_i value determines also the emission profile $\varphi_p^{(n)}(\nu)$ as the $2k$th eigenfunction of Eq. (17) with $p=p_i$. Note that modes belonging to the same branch (the quantum number n is fixed) have different p_i values for the same opacity τ and, therefore, their frequency dependences are quite different.

Finally, we point out one more important interpretation of the quantization rules. They establish the relationship be-

[4]See Eq. (23) by taking into account that $\lambda_{2k,i}=E_{2k}(p_i)$.

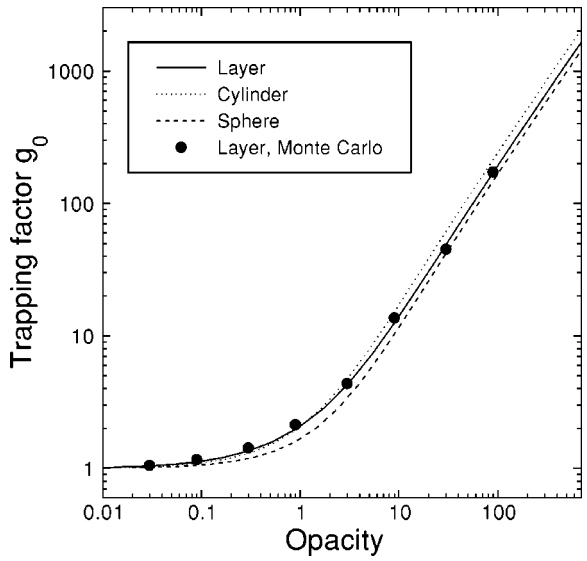

FIG. 5. Fundamental mode trapping factors $g_{0,0}$ for a layer, an infinite cylinder, and a sphere as a function of the opacity τ. For the layer with total length L, the opacity is calculated as $\tau=\kappa_0^{(D)}L$; $\tau=\kappa_0^{(D)}R$ for a cylinder or a sphere with radius R. The dots represent the results obtained by Monte Carlo simulations [13].

tween the reduced opacity $\tau_r=\kappa_0^{(D)}p^{-1}$ and the ordinary vapor cell opacity τ. For instance, in a layer, Eq. (35) reads

$$\tau/\tau_r=\pi l_z+\Delta S^{(n)}(\tau_r^{-1},\Theta=0). \tag{42}$$

One can estimate the accuracy of the developed GQT scheme with the data for the fundamental mode trapping factor g_0 (note that consideration of the lowest mode, which corresponds to the quasiparticle ground state, provides a stringent test for the accuracy of semiclassical methods). The factors g_0 obtained within the GQT are plotted in Fig. 5 for 1D geometries and are compared with results of numerical calculations (dots in Fig. 5, see also Table I). One can infer that the GQT provides values of g_0 within a 2–4 % error margin for the layer. For other higher modes with modal index $i>0$, the GQT gives substantially more accurate results.

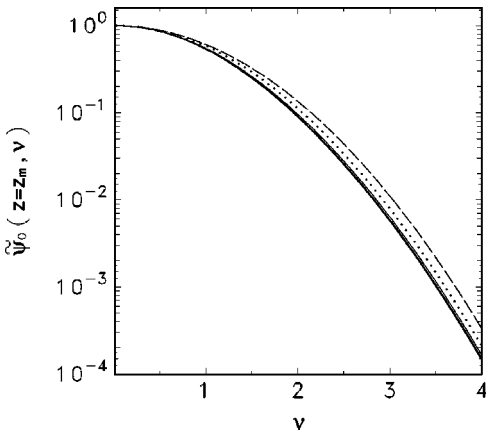

FIG. 6. Illustration of the validity for the factorization assumption, Eq. (30). A layer with total length L and opacity $\tau=3$ is considered. The frequency dependences of $\tilde{\Psi}^*_{n=0,i=0}(z_m,\nu)$ are calculated numerically with the method [23] and are plotted (solid curves) for five points $z_m=m(L/10), m=0,\ldots,4$. The dotted curve corresponds to the layer boundary; the dashed curve represents the Doppler profile $\exp(-\nu^2/2)$. All curves are normalized to unit value at the line center.

A comparison between the frequency distribution $\varphi_p(\nu)$ obtained within the GQT approach (solid curves) and the numerical evaluation (dashed curves) of the frequency distribution of excited atoms at the center of the layer for $\tau_r=2$ is given in Fig. 1. We see that numerical and analytical results are in good agreement. The assumption of mode factorization [see Eq. (30) in Sec. V], which is most essential for the semiclassical treatment, is confirmed by Fig. 6 and obtained by using numerical methods developed in [23,24] on the basis of the split-propagation technique [24].

We would like to discuss one more relevant feature of the radiation trapping phenomenon with the DFR mechanism. As mentioned above, the results of the CFR approach can be obtained within our study with the first-order perturbation theory [see the discussion of Eqs. (21) and (23)]. However, it is well known that, for large opacities, the main effects of radiation trapping processes are determined by the wings of the spectral line. From this point of view, the perturbation theory is not an adequate tool for the evaluation of trapping

TABLE I. Eigenvalues of $\lambda_{0,0}$ and $\lambda_{0,1}$ of the first two modes for a layer with total length $2L$ and their comparison with numerical results. The opacity τ is calculated as $\kappa_0^{(D)}L$.

Fundamental mode; $n=0$, $i=0$				First odd mode; $n=0$, $i=1$	
Opacity	GQT	Num. [23]	Num. [14]	Opacity	GQT	Num. [23]
1.0	0.4792	0.4520	0.4690	1.0	0.7601	0.7628
2.0	0.3149	0.3090	0.316	2.0	0.5981	0.6009
3.0	0.2301	0.2283	0.228	3.0	0.4841	0.4872
5.0	0.1450	0.1449	0.147	5.0	0.3391	0.3424
10	0.07098	0.07076	0.0713	10	0.1799	0.1824
30	0.02047	0.02039	0.0204	30	0.05333	0.05412
50	0.01190	0.01105	0.0112	50	0.02948	0.02976
70	0.007773	0.007514	0.0077	70	0.01940	0.02018
100	0.005188	0.005001	0.0047	100	0.01322	0.01329

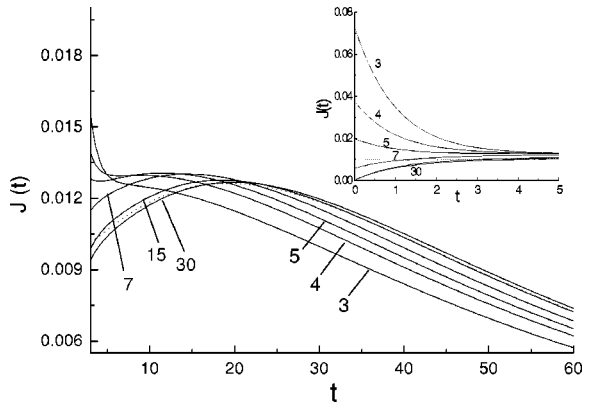

FIG. 7. Temporal behavior of the total intensity $J(t)$ of escaping radiation for a layer. Initially the layer, with total length L and opacity $\tau=30$, is excited in its central part $|z|<0.05L$. The initial frequencies ν_i of the excitation are related to the opacities $\tau_i = 30\exp[-(\nu_i-\nu_0)^2]$, which are marked close to each curve. The dotted line corresponds to the initial frequency distribution with the Doppler profile. The inset displays an enlarged view corresponding to the initial stage of the process.

factors. Indeed, Eq. (17) does not allow one to describe its solutions $\varphi_p(\nu)$ as a perturbed function in the frequency region of its exponential decrease [18], i.e., in the line wings. For this reason, the high accuracy of the CFR approach seems to be accidental. If the dispersion branch index n is positive, then the evaluation of both the dispersion functions $E_n(p)$ and the phase jumps $\Delta S^{(n)}$ within the framework of the perturbation approach is not quite accurate, as one can conclude from Figs. 2 and 4.

Continuing our discussion of the CFR approach accuracy, we address the basic structure of the emission profiles $\varphi_p^{(0)}(\nu)$ in the small opacity case. Let us consider the modified profile $\tilde{n}_{\tau\sim 0}^{(n=0)}(\nu)$ determined by Eq. (27). From the variation principle, one can easily obtain that the best choice among the Gaussian approximations $\phi_{\tau\sim 0}^{(n=0)}(\nu)\sim\exp(-a\nu^2)$ is given with $a\approx 1.46$. Such a representation is quite accurate at the line center. The modified profile at the line wings can be obtained by solving Eq. (27) in the classically forbidden region. Conventional semiclassical analysis [18] reveals a new factor in the emission profile $\varphi_{\tau\sim 0}^{(n=0)}(\nu) \sim \nu^{-1}\exp(-\nu^2)(\nu\to\infty)$ as compared with the pure Doppler profile $\exp(-\nu^2)$; the additional factor ν^{-1} in the line wings was first mentioned in [16]. Thus, we have obtained a noticeable narrowing of the emission line with simultaneous deformation of its wings due to the Doppler mechanism of the frequency redistribution. One can clearly reveal these trends in data presented in Fig. 1.

As shown above, the space relaxation constants for the CFR case and for the ground modes (with $n=0$) in the PFR case are quite similar to one another. On the other hand, the prompt relaxation of initial frequency distribution to the lowest mode (in the DFR case) occurs in the scale of the natural radiative lifetime. This can lead to specific features in the time dependence of intensity of the escaping radiation $J(t)$ under the conditions of after glow experiments. In Fig. 7, we give an example of the dependence of $J(t)$ on the center frequency ν_i of the primary spectral distribution. The atoms have been excited at the center of the layer with an initial density distribution $n^*(z,\nu,t=0)=(L\rho)^{-1}\Theta_\rho(z)\delta(\nu-\nu_i)$. Here $\Theta_\rho(z)$ is Heaviside step function that has unit value for $|z|<\rho L/2$ and zero value for $|z|>\rho L/2$. We choose the layer opacity $\tau=\kappa_0^{(D)}L=30$ and set the excitation zone index $\rho=0.1$. The total radiation intensity is connected to the total amount of the excited atoms $N(t) = \int_{-L/2}^{L/2}dz\int_{-\infty}^{\infty}d\nu\, n^*(z,\nu,t)$ by the relation $J(t) = -dN(t)/dt$. The calculations were performed using Fourier series [2,7] with the modes and trapping factors evaluated by the GQT.

A specific growth of the intensity $J(t)$ at some stage of the decay process can be considered as a result of interplay between two processes. At the first stage, $t<1$ (we remind the reader that the time unit in our study is the radiative lifetime A_{21}^{-1}), of the radiation escape, photons are emitted only from the center of the layer without absorption, and they have to fly along the optically thick path with opacity $\tau_i=\tau\exp[-(\nu_i-\nu_0)^2]$. Simultaneously, due to the radiation trapping, the spatial diffusion of the excited atoms proceeds and, at a certain moment, a considerable part of the layer becomes occupied by the excited atoms. Some fraction of the excited atoms is close to the layer borders and can emit photons outside the layer without capture. Thus, the increase of the intensity $J(t)$ is related both to the expansion of the excitation zone and to the circumstance that the main contribution to $J(t)$ arises from secondary emitted photons (see also [25]). The decrease of radiation intensity begins when the excitation zone reaches the cell boundary.[5]

Another important feature in the decay curves shown in Fig. 7 is their deformation with deviation of the initial frequency detuning ν_i from the line center ν_0. The decrease of the optical thickness τ_i for primary escaping photons leads to an increase of the initial intensity $J(t=0)$. On the other hand, since the relaxation constants $\lambda_j=E_{2k>0}$ are close to unity [see Eq. (23)], the relaxation of the initial frequency distribution to the Doppler profile leads to a coincidence of the DFR curves with the CFR curve (dashed line). For large detuning (small τ_i), however, the primary emitted photons can excite the atoms far from the layer center. Consequently, the excitation zone reaches the layer walls faster, and the layer starts to emit photons in the fundamental mode regime without any preliminary growth of the intensity.

Further PFR problems

The geometrical quantization technique developed above can be applied to a large variety of physically interesting situations. Actually, this approach can be used to analyze the entire class of phenomena for which the ν dependence of the propagator $G_{\nu\nu'}(\rho)$ can be related to a second-order differ-

[5]It is noteworthy that various types of spectral lines have different relative probabilities for a photon to escape after m elementary absorption processes. In the Lorentz line case, for instance, no increase of light emission intensity occurs.

ential operator or its Green function. We outline two examples of radiation trapping problems that can be considered with this method.[6]

The representation [26,27]

$$\overline{\kappa R}_{\nu\nu'} = \delta(\nu-\nu')\left[\kappa(\nu') + \frac{(\Delta\nu^{(D)})^2}{2}\frac{\partial}{\partial\nu'}\kappa(\nu')\frac{\partial}{\partial\nu'}\right] \tag{43}$$

is valid in the case of frequency diffusion in the spectral line when the absorption/reemission processes are regarded as essentially coherent due to the natural broadening, while the redistribution due to the Doppler effects is relatively small [2]. In a vapor medium, this situation can occur in the intermediate range of gas pressure [4] when the escape factors are determined mainly by the natural Lorentz wings of the Voigt profile. In plasma physics, the relation $\Delta\nu^{(D)} < \Delta\nu^{(L)}$ between Doppler and natural widths is typical for highly ionized gases [27].

Another important object that can be studied directly with the developed methods is radiation transfer in a system of cold atoms in a magneto-optical trap (MOT). For typical MOT conditions [6], the ratio $\Delta\nu^{(D)}/\Delta\nu^{(L)}$ is less than 0.05, and the diffusion approach [Eq. (43)] reduces the computation of the emission profile $\varphi_p(\nu)$ in modes to the study of a stationary wave equation similar to Eq. (17). Moreover, the GQT succeeds in solving the Streater equation [28], which seems to be more adequate [6] for describing radiation effects in cold atoms than the Payne equation [4] [Eq. (1)]. The Streater theory accounts for the fact of instantaneous (Rayleigh) photon scattering by introducing the additional term

$$\int_{-\infty}^{\infty} d\nu' \int_{\Omega} d^3r' \left[\overline{\kappa R}_{\nu\nu'} - \frac{1}{\kappa}\kappa(\nu)\kappa(\nu')\right] \times \tilde{G}_{\nu'}(|\vec{r}-\vec{r}'|)\frac{\partial}{\partial t}n^*(\vec{r}',\nu',t) \tag{44}$$

on the right-hand side of Eq. (1).

In particular, for the Streater problem [28], the dispersion law $E_0(p)$ of the quasiparticle in the fundamental branch can be obtained:

$$E_0^{-1}(p) = \frac{1}{\pi}\int_{-\infty}^{\infty}\frac{dx}{1+x^2}\left[1-\frac{\kappa^{(L)}(x)}{p}\arctan\left(\frac{p}{\kappa^{(L)}(x)}\right)\right]^{-1},$$

$$\kappa^{(L)}(x) = \frac{\kappa_0^{(L)}}{1+x^2}. \tag{45}$$

Thus, the GQT allows us to analytically evaluate the entire spectrum of both the modes and the corresponding radiation trapping factors in a MOT that was studied experimentally in [6]. We plan to consider this very important problem in a separate publication.

VII. CONCLUSIONS

Integro-differential equations describing the radiation energy transfer belong to a special class of equations that covers a much richer and broader range of physical phenomena than the local diffusion equations of the Fokker-Planck type. In this paper, we have presented an analytical, rather accurate (albeit approximate), method treating the basic trapping equation as a generalized wave (diffusion) equation. Namely, we have exploited the semiclassical geometrical quantization technique (GQT) for such problems.

Although our treatment has been applied mainly to the case of the pure Doppler redistribution function, the results obtained are expected to be quite general. The semiclassical study and independent numerical calculations reveal the *qualitative* feature of the trapping equations with PFR, namely the high accuracy of the mode factorization assumption expressed by Eq. (30) and interpreted as an approximate separation of the spatial and frequency variables. This allows one to reduce the general task to consideration of two parametrically coupled problems.

(i) The first problem can be obtained after the spatial Fourier transform of the 4D trapping equation kernel *in infinite space* is performed. Essentially, this problem deals with the 1D spectral problem in the frequency space. The spatial Fourier variable $\vec{p}$ enters the wave like 1D equation obtained as a parameter and only with its absolute magnitude $p=|\vec{p}|$. This spectral problem determines both the emission profiles $\varphi_p^{(n)}(\nu)$ and the dispersion laws $E_n(p)$ of modes as a function of p. The frequency quantum number n (which must be even) distinguishes different dispersion branches (excited levels) of that 1D equation.

(ii) The second part deals with the spatial variables of the trapping equation and relates the Fourier parameter $\vec{p}$ to the momentum of an associated quasiparticle moving in the space and confined in the vapor cell by the effective potential walls. Remarkably, the dispersion law $E_n(p)$ for this quasiparticle is determined from the first part of the task described above. The total density of atoms at the point $\vec{r}$, $N_i(\vec{r})$, satisfies the conventional Holstein trapping equation with emission profile $\varphi_p^{(n)}(\nu)$. The relevant parameter p can be determined within the GQT [10,11] by using generalized quantization rules. The effective radiation trapping constant $\lambda_{n,i}=E_n(p_i)$ corresponding to the mode (n,i) can be calculated analytically. A comparison of the results obtained with available numerical data indicates the high accuracy of the GQT.

Therefore, we have obtained an answer for the long-standing problem concerning the accuracy of the complete frequency redistribution approximation in the case of Doppler spectral redistribution. The statement derived previously from various numerical simulations of the discussed processes for the simplest experimental configurations of vapor cells, namely that *CFR gives the trapping factors for fundamental mode within a 12% accuracy level*, has been con-

[6]A wide range of corresponding problems can be found in plasma physics [3] in the theory of electron redistribution over the space and energy variables via the linear transport Boltzmann equation.

firmed in our study. We have also explained a noticeable discrepancy between the actual emission profiles and the Doppler one. It is shown that the behavior of the emission profile in the wings of the spectral line is connected to the behavior of eigenfunctions for the perturbed oscillator problem in the classically forbidden region. From this result, it follows that straightforward perturbation theory cannot be applied to the determination of the wing effects. This explains the deviations between some numerical observations [13] and theoretical predictions [29] pointed out in [13].

The geometrical quantization technique turns out to be a quite powerful technical tool for solving the radiation trapping problems both for CFR theory and for more realistic conditions of partial frequency redistribution. As the next stage in our study of the radiation trapping, we plan to apply this method to radiation trapping phenomena in the cases in which the diffusion mechanism [26,27] of the line wing formation plays an important role. The corresponding experimental situations take place in different branches of physics. As an example, we mention the phenomena taking place in plasma [27,30] and the processes relevant in a system of cold atoms in magneto-optical traps [6].

It should be also noted that the solutions of certain linear trapping problems play an important role in the construction of fast analytical algorithms for investigation of the effects described by nonlinear radiation transfer equations [31,32]. The GQT method developed provides a powerful universal tool for obtaining analytical information required in those studies [32].

ACKNOWLEDGMENTS

We are very grateful to NATO for financial support via the Linkage and Networking program (under Grant No. PST.CLG 975350). We are pleased to acknowledge useful discussions with Dr. A.F. Molisch, who kindly provided us also with the updated data of numerical calculations by the method presented in [14].

APPENDIX: A STUDY OF THE GENERALIZED 4D WAVE EQUATION BY THE SEMICLASSICAL APPROACH

We start by reiterating the basic Eq. (15) for the jth eigenmode,

$$\hat{L}_{\nu}[-\lambda_j+1+W_{\Omega}]\tilde{\Psi}_j^*(\vec{r},\nu)=\Phi(-i\vec{\nabla},\nu)\tilde{\Psi}_j^*(\vec{r},\nu). \tag{A1}$$

Conventionally, a semiclassical approach implies the eigenfunction ansatz in the form of a product of rapidly and slowly varying functions [18,33]:

$$\tilde{\Psi}_j^*(\vec{r},\nu)\sim A_j(\vec{r},\nu)\exp[\pm\imath S_j(\vec{r},\nu)]. \tag{A2}$$

The quantity $S_j(\vec{r},\nu)$, conventionally referred to as a shortened action, obeys the Hamilton-Jacobi equation [33]

$$H^{(4D)}(p_{\nu},\nu;\vec{p})=0.5\,\frac{1+\lambda_j-W_{\Omega}}{1-\lambda_j+W_{\Omega}},$$

where

$$p_{\nu}=\frac{\partial}{\partial\nu}S_j(\vec{r},\nu),\quad \vec{p}=\vec{\nabla}_r S_j(\vec{r},\nu); \tag{A3}$$

$$H^{(4D)}(p_{\nu},\nu;\vec{p})=\frac{1}{2}p_{\nu}^2+\frac{1}{2}\nu^2+\frac{1}{1-\lambda_j+W_{\Omega}}V_p(\nu),$$

$$p=|\vec{p}|. \tag{A4}$$

In solving Eq. (A3) for S_j, we apply the Jacobi method [20]. Namely, the function $H^{(4D)}$ entering Eq. (A4) determines a Hamiltonian function over the phase space $\{p_{\nu},\nu;\vec{p},\vec{r}\}$ for the 4D classical system that we associate with a 4D quasiparticle. The Hamiliation $H^{(4D)}$ gives rise to the quasiparticle trajectories $\{\nu(t),\vec{r}(t)\}$ via the Hamiltonian motion equations

$$\frac{d}{dt}\vec{p}=-\frac{\partial H}{\partial\vec{r}}=0,\quad \frac{d}{dt}\vec{r}=\frac{\partial H}{\partial\vec{p}}=\frac{1}{1-\lambda_j+W_{\Omega}}\frac{\partial}{\partial p}V_p(\nu)\frac{\vec{p}}{p}, \tag{A5}$$

$$\frac{d}{dt}p_{\nu}=-\frac{\partial H}{\partial\nu}=-\nu-\frac{1}{1-\lambda_j+W_{\Omega}}\frac{\partial}{\partial\nu}V_p(\nu),$$

$$\frac{d}{dt}\nu=\frac{\partial H}{\partial p_{\nu}}=p_{\nu}. \tag{A6}$$

The trajectories $\{\nu(t),\vec{r}(t)\}$ play the role of rays along which the corresponding wave fronts are propagating.[7] Accordingly, the phase factors $S_j(\vec{r},\nu)$ are obtained as an action integral over these rays [20]:

$$S_j(\vec{r},\upsilon)=\int^{\vec{r},\upsilon}[\vec{p}\,d\vec{r}+p_{\nu}d\nu]. \tag{A7}$$

From Eqs. (A5), it is clear that the momentum $\vec{p}$ remains constant within the vapor cell Ω (where $W_{\Omega}=0$). In other words, the quasiparticle moves freely (see Fig. 3) inside Ω. The region outside Ω, where W_{Ω} is assumed to be very large, is forbidden for classical motion[8] and the quasiparticle

[7]For a detailed discussion of the relation between the quasiparticle rays and the wave fronts, see [11,21].

[8]As it follows from Eq. (A3), the positive Hamiltonian $H^{(4D)}$ defined by Eq. (A4) has to get the negative magnitude -0.5 if $W_{\Omega}=\infty$.

is reflected by the cell boundary $\partial\Omega$. These reflections change only the orientation of the momentum $\vec{p}$. Equation (A6) determines the quasiparticle motion with respect to the frequency. It is not influenced by the space motion, since the p magnitude entering these equations does not vary. Therefore, in the Hamiltonian $H^{(4D)}$, the spatial and frequency parts are independent. This statement leads to the conclusion that the phase S_j is the sum of two independent parts $S_j = S_n(\upsilon) + S_i(\vec{r})$, which is equivalent to factorization, Eq. (30), of the eigenmode Ψ_j^*.

[1] A. G. Mitchell and M. W. Zemanski, *Resonance Radiation and Excited Atoms* (Cambridge University Press, Cambridge, 1961).

[2] A. F. Molisch and B. P. Oehry, *Radiation Trapping in Atomic Vapours* (Oxford University Press, Oxford, 1998).

[3] L. M. Biberman, V. S. Vorobjev, and I. T. Yakubov, *Kinetics of Nonequilibrium Low-Temperature Plasma* (Plenum, New York, 1987).

[4] M. G. Payne, J. E. Talmage, G. S. Hurst, and E. B. Wagner, Phys. Rev. **181**, 97 (1969).

[5] A. Corney, *Atomic and Laser Spectroscopy* (Oxford University Press, Oxford, 1977).

[6] A. Fioretti, A. F. Molisch, J. H. Muller, P. Verkerk, and M. Allegrini, Opt. Commun. **149**, 415 (1998).

[7] T. Holstein, Phys. Rev. **72**, 1212 (1947); **83**, 1159 (1951).

[8] V. V. Ivanov, *Transfer of Radiation in Spectral Lines*, NBS Special Publ. No. 385 (U.S. GPO, Washington, D.C., 1973).

[9] C. van Trigt, Phys. Rev. **181**, 97 (1969); Phys. Rev. A **1**, 1298 (1970); **4**, 1303 (1971); **13**, 726 (1976).

[10] N. N. Bezuglov, A. F. Molisch, A. N. Klucharev, F. Fuso, and M. Allegrini, Phys. Rev. A **57**, 2612 (1998).

[11] N. N. Bezuglov, A. F. Molisch, A. N. Klucharev, F. Fuso, and M. Allegrini, Phys. Rev. A **59**, 4340 (1999).

[12] N. N. Bezuglov and B. V. Taratin, Opt. Spektrosk. **84**, 893 (1998) [Opt. Spectrosc. **84**, 807 (1998)].

[13] A. Hishikawa, T. Fujimoto, and P. Erman, Phys. Rev. A **52**, 189 (1995).

[14] A. F. Molisch, G. J. Parker, B. P. Oehry, W. Schupita, and G. Magerl, J. Quant. Spectrosc. Radiat. Transf. **53**, 269 (1995).

[15] V. V. Ivanov and V. V. Schneeveis, Astrofizika **12**, 245 (1976).

[16] C. van Trigt, Phys. Rev. A **13**, 726 (1976).

[17] M. I. D'yakonov and V. I. Perel', Zh. Éksp. Teor. Fiz. **47**, 1483 (1964) [Sov. Phys. JETP **20**, 997 (1965)].

[18] L. D. Landau and E. M. Lifshitz, *Quantum Mechanics* (Pergamon, New York, 1977).

[19] N. N. Bezuglov and B. V. Taratin, Opt. Spektrosk. **86**, 360 (1999) [Opt. Spectrosc. **86**, 310 (1999)].

[20] V. I. Arnold, *Mathematical Methods of Classical Mechanics* (Springer, Berlin, 1978).

[21] J. B. Keller, *A Geometrical Theory of Diffraction*, in *Proceedings of the Symposia on Applied Mathematics* (McGraw-Hill, New York, 1958), Vol. VIII, p. 27.

[22] I. C. Percival, Adv. Chem. Phys. **36**, 1 (1977).

[23] A. K. Kazansky, N. N. Bezuglov, A. F. Molisch, F. Fuso, and M. Allegrini (unpublished).

[24] A. K. Kazansky and N. N. Bezuglov, J. Phys. B **33**, 99 (2000).

[25] P. Wiorkowski and W. Hartman, Opt. Commun. **53**, 245 (1985).

[26] H. Frisch and C. Bardos, J. Quant. Spectrosc. Radiat. Transf. **26**, 119 (1981).

[27] A. E. Suvorov, Zh. Éksp. Teor. Fiz. **92**, 444 (1987) [Sov. Phys. JETP **65**, 251 (1987)].

[28] A. Streater, J. Cooper, and W. Sandle, J. Quant. Spectrosc. Radiat. Transf. **37**, 151 (1987).

[29] V. I. Perel' and I. V. Rogova, Zh. Éksp. Teor. Fiz. **65**, 1012 (1973) [Sov. Phys. JETP **38**, 501 (1974)].

[30] V. Makhrov, A. Yu. Sechin, and A. N. Starostin, Zh. Éksp. Teor. Fiz. **97**, 1114 (1990) [Sov. Phys. JETP **70**, 623 (1990)].

[31] N. N. Bezuglov, A. N. Klucharev, and T. Stacewicz, Opt. Spektrosk. **77**, 342 (1994) [Opt. Spectrosc. **77**, 304 (1994)].

[32] N. N. Bezuglov, A. N. Klucharev, A. F. Molisch, M. Allegrini, F. Fuso, and T. Stacewicz, Phys. Rev. E **55**, 3333 (1997).

[33] M. V. Fedoryuk, *Sovremennnye Problemy Matematiki (Itogi Nauki I Tekhniki) (Modern Problems of Mathematics)* (VINITI, Moscow, 1988), Vol. 34, pp. 5–56.